INVESTIGATION OF CLOUD PROPERTIES AND ATMOSPHERIC STABILITY WITH MODIS

QUARTERLY REPORT FOR JUL-SEP 1995

Paul Menzel
NOAA/NESDIS at the University of Wisconsin

Contract NAS5-31367

ABSTRACT

In the past three months, considerable progress was made toward beta software deliveries, the spectral and radiometric performance of the MAS (MODIS Airborne Simulator) were characterized, and the SCAR-B field experiment was supported daily with real time analysis of the biomass burning and associated smoke in South America.

TASK OBJECTIVES

Software Development

Work continues on evolving the three software packages (cloud mask, cloud top properties, and atmospheric profiles) from AVHRR, HIRS, and MAS data to MODIS data. Beta 3 software was delivered to the SDST by the end of October 1995. For the cloud mask, several data sets in different land/ocean and winter/summer regimes were developed with AVHRR and MAS data; feedback from other users is now being solicited. A cloud mask over land with AVHRR/HIRS LAC (local area coverage) data was delivered in the second quarter of 1995. High resolution cloud masks using MAS 50 channel data over different atmospheric and surface regimes (a tropical data set from the Gulf of Mexico experiment (6 and 13 January 1995) and an Arctic data set from BOREAS (21 April 1995) were also processed within the last quarter and will be distributed next quarter.

Evolving the ATBDs

The UW ATBDs will be revised to include information from the continuing MAS, AVHRR, HIRS, and GOES cloud investigations. Another version of the ATBDs will be drafted in early 1996.

Algorithm Definition

Processing and testing of the cloud parameter algorithms (mask, temperature, phase, height, and amount) will continue using the MAS data at UW. Algorithms for atmospheric total column amount (ozone, precipitable water vapor, and stability) and profiles (temperature and moisture) will be developed using the GOES-8 and HIRS data from the field experiment completed with the MAS and HIS in January.

Global Cloud Study

Pre-MODIS cloud studies will continue via the global cloud census with HIRS data now in its seventh year.

MODIS Infrared Calibration

Postlaunch procedures for validating MODIS radiances will continue to be refined; an initial demonstration with GOES-8 using underflights of the MAS and HIS was successful in January. Prelaunch calibration of the MODIS infrared channels requires considerable testing to characterize detector to detector and band to band cross talk, detector non-linear response, stray radiation, scan mirror emissivity variations with angle and wavelength, angle dependence of background radiation, and other effects. The Engineering Model thermal vacuum tests are being studied to reveal answers and questions.

WORK ACCOMPLISHED

MODIS Software Development and Cloud Mask Delivery

Considerable effort was spent in preparation for the MODIS Beta software deliveries, culminating in an updated Beta 3 cloud mask algorithm transfer to the SDST in September. Beta software development involved several steps:

(1) Computing MODIS IR band transmittance profiles.

Hal Woolf created a new regression-based MODIS IR band transmittance model, using the MODIS specification spectral response data delivered by SDST in Sep 94. The model was developed using a 32 atmosphere dependent set, and FASCODE transmittance profile computations at 6 equally spaced sensor zenith angles from nadir to sec (2.25). This method has been used for other sensors including HIRS, GOES, and AVHRR. A profile of transmittances at 40 standard pressure levels from 0.1 (space) to 1000 mb was derived. Before this model was finished, development work was done using a 0.1 wavenumber fast model, where the resulting transmittances were weighted with the MODIS spectral responses.

(2) Conversion of simulated MODIS IR band radiance (W/m^2/ster/{symbol 109 \f "Symbol" \s 12}m) to brightness temperature (K), and then to UW-preferred radiance units (mW/m2/ster/cm-1).

MODIS radiances are stored in radiance units per wavelength interval; in the infrared it is common to use radiances in units per wavenumber interval. Thus code was developed to convert MODIS radiances to brightness temperature, and then from brightness temperature to UW-preferred radiance units. The algorithm uses a computed central wavenumber for each MODIS IR band and regression coefficients that predict the true brightness temperature from the monochromatic brightness temperature over the temperature range 180 to 320K.

(3) Reading the simulated MODIS Level-1B and geolocation data sets.

Simulated MODIS Level-1B data were received in last half of September. Significant effort was required to use the data with the current UW MODIS algorithms. R. Hucek of the MODIS SDST was helpful in sorting out some of the idiosyncrasies of the simulated data. All of the UW MODIS algorithms are now able to read and process the MODIS simulated scan cubes. However it should be noted that scientific value of the simulated data is low for our cloud and atmospheric profile products, since no clouds are included and clear-sky radiances appear to be suspect. We will continue to use our own MODIS-like simulated data, created from other sensors such as MAS, HIRS, and AVHRR for testing and developing our MODIS algorithms.

(4) Utilizing the PGS and MODIS API toolkits.

The Beta 3 delivery uses the toolkits for opening and closing files, accessing MODIS data, and message logging. While some learning time was required, it was eventually possible to use the PGS and MODIS API toolkits for all the UW MODIS algorithms.

(5) Creating MODIS product files in HDF.

MODIS product files were created using the Interface Control Documents (ICDs) as a guide. As far as possible we attempted to duplicate the structure of the MODIS products outlined in the ICDs.

Since the simulated radiances were of a clear atmosphere only, the cloud mask results were not high confidence clear for all pixels. Two main reasons for the lower confidence clear scenes were identified: (a) The first involves unrealistic radiances over water. Calculated .87 micron channel reflectances were higher over water than .66 micron reflectances. This led the reflectance ratio test to flag many of the water scenes as low confidence clear. The SDST has identified the problem in their simulation. (b) There was a resolution mis-match between the land/sea mask used in the data simulation and the cloud mask algorithm. A 4 km land/sea mask was used as part of the simulated radiance generation, whereas the cloud mask relies upon a 1 km land/sea mask to determine the correct processing path. The difference in resolution results in lower confidence clear values along the land/water boundaries.

Beta deliveries for the remaining UW MODIS products (atmospheric profiles, cloud top properties) will occur in October.

MAS 50 Channel Cloud Mask

In preparation for the MODIS day-1 cloud mask product, data from the 50 channel MODIS Airborne Simulator (MAS) is being used to develop a multispectral cloud mask algorithm. The spectral tests used to determine an unobstructed confidence level rely on radiance (temperature) thresholds in the infrared and reflectance thresholds in the visible. These thresholds vary with surface type, atmospheric conditions (moisture, aerosol, etc.) and viewing geometry. A necessary part of the algorithm development is to characterize the individual spectral test thresholds as a function of these variables.

The relatively small geographical coverage of MAS data sets make it difficult to study global spectral threshold regimes; however, with global observations provided by the coarser spectral and spatial resolution AVHRR/HIRS data sets, a cloud mask algorithm can be determined which takes advantage of the strengths of each instrument. For example, an unobstructed CO_2 channel (13.9 micron) threshold of 245 K was set by examining global clear sky HIRS observations as determined from Collocated HIRS/2 and AVHRR ProductS (CHAPS) processing.

Using the information provided by both global and regional data sets, an initial algorithm has been developed to test upon MAS high spectral resolution data in different ecosystem regimes. Both a tropical ocean scene (Gulf of Mexico, 13 January 1995) and a polar land scene (Alaska, 21 April 1995) have been chosen to test the algorithm. Both data sets and results will be released for distribution to the SDST in November.

SCAR-B Support

During the SCAR-B field program from mid-August to mid-September, UW-Madison provided the mission scientists in Brazil with GOES-8 satellite imagery, GOES ABBA fire products, meteorological observations, and NMC model output via the UW-Madison SSEC SCAR-B web site. The web site consisted of three components: GOES-8 imagery loops (3-hourly visible and infrared), GOES-8 ABBA products, and the McWEB forecasting tool. This interactive tool allowed the scientists to access meteorological information as well as satellite imagery and satellite derived fire products from the Mission Operations Center at IBAMA. The web site provided daily plots of fire locations at peak burning times (11:45, 14:45, 17:45, 20:45 UTC) for the region extending from approximately 40 to 70°W and from the equator to 30°S. A text summary of daily peak fire statistics from the GOES-8 ABBA was also available. The site also contained a morning (11:45 UTC) and afternoon (17:45 UTC) GOES-8 visible image with outlines depicting the areal extent of smoke/aerosol coverage based on an analysis of visible and infrared imagery.

Collaboration with Snow Mask Group

A dialogue was opened at the snow and ice workshop held at GSFC on 13-14 September and will be continued between the snow mask algorithm developers, led by Dorothy Hall, and the UW cloud mask team. Many issues need to be agreed upon by the two groups, including which algorithm should run first during operational processing.

Split Window Cloud Studies

MAS, GOES-8, HIS, and AVHRR data are being used in an investigation of negative 11 micron minus 12 micron (T11-T12) occurrences. MAS and HIS comparisons (January 1995 data set) suggest that MAS T11-T12 differences are biased negative. MAS blackbody emissivity corrections reduce the magnitude, however MAS T11-T12 remains negatively biased to HIS T11-T12. GOES-8 and AVHRR T11-T12 also exhibit negative differences. These show temporal and spatial consistency in scenes of vigorous convective growth, lending credibility to the hypothesis that negative differences are related to cloud microphysics. Observations by MAS and HIS of vigorous convective growth are still needed as a means of corroborating GOES-8 observations. A poster on this topic will be presented next January at the 8th Conference on Satellite Meteorology and Oceanography

DATA ANALYSIS

Cloud Mask Test Data Set Delivery

A global 1-day cloud mask data set has been created using AVHRR (Advanced Very High Resolution Radiometer) GAC (Global Area Coverage) measurements and delivered to the SDST for distribution. The data set was produced for the purpose of identifying problems associated with building the global MODIS cloud mask algorithm. A robust method must readily adjust to variations in illumination, surface properties, ecosystems, and atmospheric temperature and humidity structure. It is emphasized that this effort is only preliminary in this respect.

The cloud mask algorithm utilizes visible and infrared spectral tests as well as spatial uniformity information and is divided into 7 conceptual domains; daytime land surface, daytime water, nighttime land, nighttime water, desert (daytime only), and daytime and nighttime polar regions. Ancillary data sets include the 10-minute Olson World Ecosystems and USGS 1 km land/sea tag files. No attention has been given to the nighttime desert and polar regions to date. Currently, the nighttime land algorithm is substituted in both cases.

GAC data has a nominal spatial resolution of 4 km where every third scan line and an average of 4 out of every 5 pixels along each scan are used. Fourteen orbits of data collected on 16 March 1994 from the NOAA-14 spacecraft were processed. The delivery includes the orbit data files, output 32 bit files as described in the cloud mask ATBD and output visualization files which allow the user to trace the cloud mask processing path and visualize test results in the satellite projection. As with the previous test data set deliveries, both the orbit data files and the output visualization files can be displayed by the MERLIN software package, which is freeware available from the SDST. Figure 1 is an example of a partial GAC orbit from 16 March 1995 covering the region from the North Pole all the way south across Antarctica. Instrument observations, processing path, a sample of the individual test results and the final cloud mask confidence level product are shown. Comments and suggestions on the test data sets are readily encouraged.

Comparison of ATSR SST to Surface Measurements

Data acquired during the OTIS (Ocean Temperature Interferometer Sensing) experiment in the Gulf of Mexico in January 1995 were analyzed to determine the agreement between ATSR SST and surface (R/V Pelican) measurements of SST. ATSR 1-km resolution data was provided by Ian Barton at CSIRO. An ATSR scene from January 16 was used in the analysis. The ATSR overpass was at 1713 UTC, while the Pelican traversed the region covered by the ATSR pass between 0130 and 0800 UTC. A simple cloud mask based on reflectance, window brightness temperature, and 11-12 micron brightness temperature thresholds was used for cloud screening. Once the clear pixels in the ATSR scene were identified, the ship track was overlaid on the ATSR scene to determine collocation. Fifteen collocation points were found; however 5 of these points were either cloud covered in the ATSR image, or at the edge of clouds. The ATSR data showed excellent agreement with surface measurements of SST derived from the AERI instrument. The RMS bias between ATSR and AERI was 0.02 K, while the RMS bias between ATSR and the R/V Pelican surface skimmer SST was 0.16 K. Further analysis of these data will be done as part of a demonstration of our capability for in-orbit validation of the MODIS IR bands.

MAS Infrared Calibration

Characterizing MAS calibration continues. This summer, spectral response measurements for all 50 MAS channels were made at the Ames Research Center (ARC) calibration facility. A one quarter meter single grating monochromator with a light source consisting of a 100 watt tungsten halogen lamp and a 100 watt Nernst glow bar were used for the measurements. The MAS output and calibrated reference detector signals were recorded at the grating monochromator step rate. Dan LaPorte and Chris Moeller participated in the experiment design and measurements at ARC in July. A finalized set of measurements were produced at ARC in August. The MAS infrared channel (26-50) measurements have been post-processed at the UW. Random noise in the calibrated reference detector data was reduced by fitting the reference data with a 2nd order function. Spectral absorption features were superimposed on this function using FASCOD3P transmittances (using laboratory ambient conditions). The MAS output and noise reduced reference function data were then ratioed. A smoothing filter (Savitzky-Golay) was applied and the data were normalized to the maximum response in each channel. The normalized SRF data (Figure 2) are much improved over the Stennis Space Center SRF data set (8/94). Noise in the SRF curves is much reduced and spectral features due to atmospheric attenuation are effectively removed from the curves. A similar post-processing procedure is planned for the MAS reflectance channels (1-25).

MAS calibration blackbody emissivity has been estimated for the infrared atmospheric window channels 31 (3.7 micron), 32 (3.9 micron), 42 (8.6 micron), 45 (11 micron) and 46 (12 micron). A laboratory data set of MAS viewing the well calibrated Advanced Kinetics Extended Area Blackbody Source was used for this work. Previously, an assumption of unit emissivity was used for all MAS infrared calibration. However, comparisons with High-resolution Interferometric Sounder (HIS) data have indicated that this assumption caused systematic error in the MAS absolute calibration for earth-atmosphere scene temperatures. Estimated emissivities along with the brightness temperature correction for typical ocean and cloud scene temperatures are shown in Table 1. The correction is a function of both emissivity and MAS instrument temperature. MAS spectrometer head temperature (typically 0 to -10{symbol 176 \f "Symbol" \s 12}C) is monitored inflight and is currently being used to characterize the MAS instrument temperature. Laboratory measurements of MAS blackbody reflectivity are planned for the next quarter. Those measurements will be compared to the emissivity estimates listed in Table 1.

The normalized SRF data and emissivity estimates are being incorporated into MAS infrared absolute calibration. New comparisons between MAS and the High-resolution Interferometric Sounder (HIS) data have been made using clear Gulf of Mexico scene data collected in January 1995. The comparisons are shown in Table 2. Non-unit emissivity changes MAS-HIS biases from positive to negative for longwave infrared channels (42, 45, 46), placing them closer to the shortwave infrared channel 32 bias. The remaining bias may be due to error in the representation of the MAS instrument temperature. Future thermal vacuum chamber laboratory measurements and additional inflight monitoring will reduce MAS instrument temperature uncertainty.

Biomass Burning in South America in 1995

Preliminary GOES-8 ABBA results obtained during SCAR-B (15 August - 15 September 1995) suggest that the peak burning time is in the middle of the afternoon (1745 UTC). The number of fires detected at 1745 UTC is 2 to 4 times greater than that observed 3 hours earlier or later and 20 times greater than that observed at 1145 UTC. The majority of the fire activity is concentrated along the perimeter of the Amazon in the Brazilian states of Para, Mato Grosso, Amazonas, and Rondonia. There is also considerable activity in Bolivia, Paraguay, and Northern Argentina. Although the burning pattern is similar to that observed with the GOES-7 ABBA in 1988, the improved spatial resolution available with GOES-8 provides much greater detail concerning fire activity and other surface features (Menzel and Prins, 1995). As in previous years, large smoke palls were identified in the GOES-8 visible imagery. During SCAR-B smoke was evident over a large portion of the continent east of the Andes Mountains. A large smoke pall covering over 4 million km^2 was observed from 21 August through 11 September. At the height of this burning period the smoke pall extended over nearly 7 million km^2. Transport over the Atlantic Ocean was observed on 13 days during the SCAR-B field program. On at least two days a thin plume of smoke was tracked to the Prime Meridian. The burning practices and meteorological conditions which contributed to this episode are nearly identical to ones which resulted in a similar smoke pall observed during the last week of August 1988.

PAPERS

Ackerman, S. A., K. I. Strabala, R. A. Frey, C. C. Moeller and W. P. Menzel, 1995: Cloud Mask for the MODIS Airborne Simulator (MAS): Preparation for MODIS. Accepted for the 8th Conference on Satellite Meteorology and Oceanography to be held in January and for the AGU Fall Meeting, Science and the First EOS Platform, EOS-AM1 session to be held in December.

Gumley, L.E., and M.D. King, 1995: Remote Sensing of Flooding in the U.S. Upper Midwest during the Summer of 1993. *Bull. Am. Met. Soc.*, **76**, 933-943.

Moeller, C.C., S. A. Ackerman, K. I. Strabala, W. P. Menzel and W. L Smith, 1995: Negative 11 micron minus 12 micron brightness temperature differences: A second look. Accepted as a poster for the 8th Conference on Satellite Meteorology and Oceanography to be held in January.

King, M. D., W. P. Menzel, P. S. Grant, J. S. Myers, G. T. Arnold, S. Platnick, L. E. Gumley, S. Tsay, C. C. Moeller, M. Fitzgerald, K. S. Brown, and F. Osterwisch, 1995: Airborne scanning spectrometer for remote sensing of cloud, aerosol, water vapor and surface properties. Submitted to Jour. Atmos. and Oceanic Tech.

Smith, W. L., R. O. Knuteson, H. E. Revercomb, W. Feltz, H. B. Howell, W. P. Menzel, N. Nalli, O. Brown, J. Brown, P. Minnett, and W. McKeown, 1995: Observations of the infrared radiative properties of the ocean - Implications for the measurement of sea surface temperature via satellite remote sensing. Accepted by Bull. Amer. Meteor. Soc.

MEETINGS

Chris Moeller and Dan LaPorte participated in the MAS spectral response measurements performed at Ames Research Center on 10-13 July.

Dan LaPorte attended the Calibration Peer Review held at Santa Barbara, CA on 13-14 September.

Steve Ackerman attended the snow and ice workshop held at GSFC on 13-14 September.

Steve Ackerman attended the SASS meeting held at Ames Research Center on 29-31 August.

Dan LaPorte attended the Calibration Workshop held in Wallops Island, VA the week of 7 August .

Paul Menzel attended the review of SDST and MCST at GSFC on 17-18 July.

TABLE 1. MAS blackbody emissivity and emissivity correction impact.

MAS channel	Central wavelength (μm)	Estimated blackbody emissivity	Ocean scene uncorrected temperature (K)	Ocean scene emissivity corrected temperature (K)	Cloud scene uncorrected temperature (K)	Cloud scene emissivity corrected temperature
31	3.74	0.978	293.2	292.9	257.1	257.5
32	3.90	0.980	291.6	291.3	241.2	242.5
42	8.59	0.942	291.9	290.8	211.7	218.3
45	11.01	0.939	294.1	292.8	213.8	219.2
46	11.97	0.937	293.4	292.0	214.5	219.7

TABLE 2. MAS window region surface temperature measurements in Kelvin compared with HIS temperature measurements derived from HIS spectra integrated over the MAS spectral response functions.

MAS channel	Central wavelength (μm)	*HIS-derived* temperature (K)	*MAS-derived* uncorrected temperature (K)	*MAS-derived* emissivity corrected temperature (K)	Uncorrected ΔT (K)	Emissivity corrected ΔT (K)
32	3.90	293.4	292.3	292.0	-1.1	-1.4
42	8.59	292.2	292.7	291.3	0.5	-0.9
45	11.01	293.9	294.9	293.3	1.0	-0.6
46	11.97	293.1	294.3	292.6	1.2	-0.5

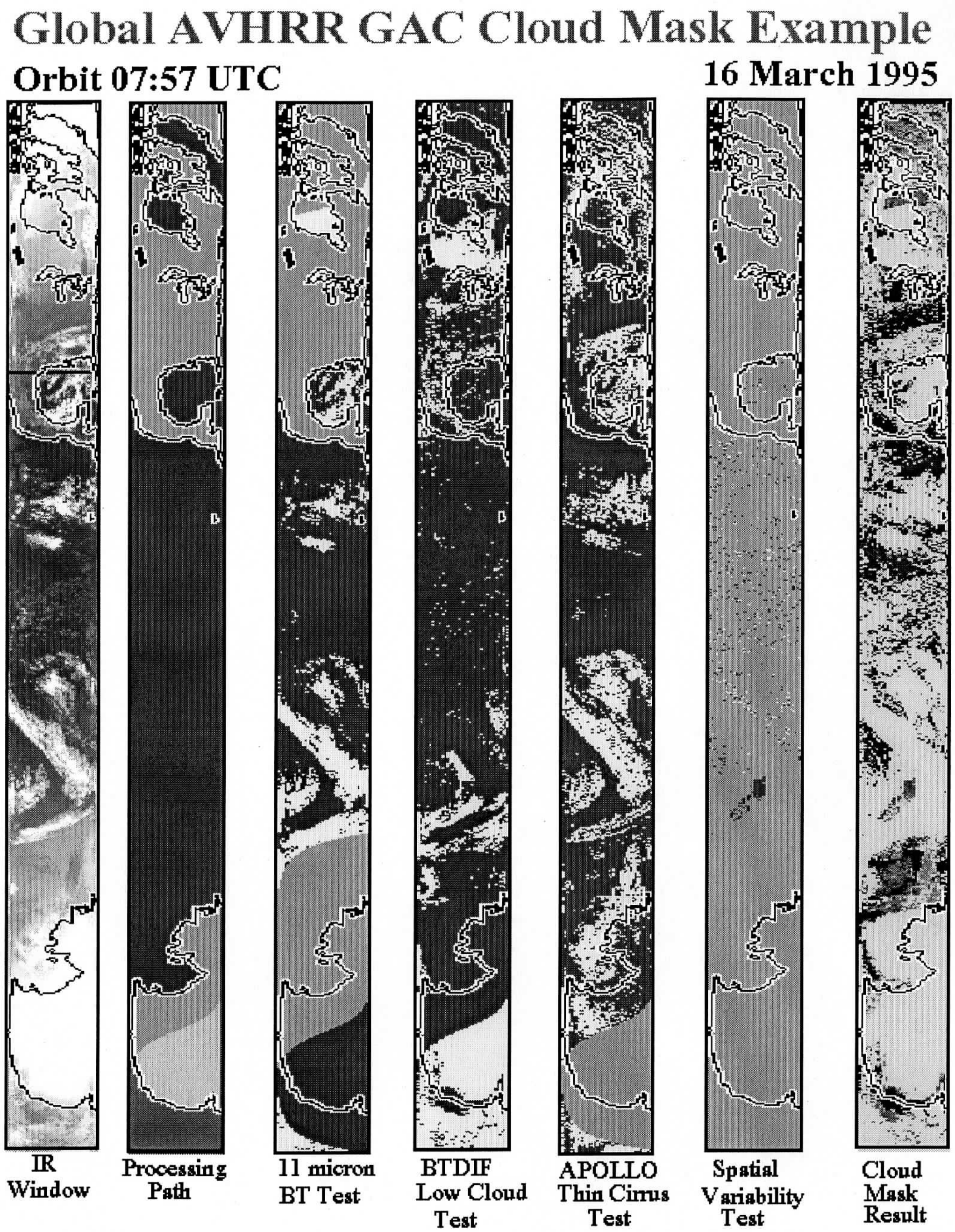

Figure 1. Partial AVHRR GAC orbit depicting 11 micron observations (left image), cloud mask processing path (second image to the left), individual cloud mask test results (middle 4 images) and resultant cloud mask (right image). Different threshold regimes are outlined by the processing path image; for instance, the darkest region indicates that the nighttime ocean algorithm was used, whereas the lightest regions represent the daytime land regime. The individual test results are color coded gray (test not applied), white (test failed - lower confidence clear) and black (test passed - higher confidence clear). The cloud mask result, which is a combination of the individual tests, is shaded light to dark representing low to high confidence clear.